

# Treating Electrostatic Shielding at the Surface of Silica as Discrete Siloxide•Cation Interactions

Mathai Mammen, Jeffrey D. Carbeck, Eric E. Simanek, and George M. Whitesides\*

Contribution from the Department of Chemistry and Chemical Biology, Harvard University, 12 Oxford Street, Cambridge, Massachusetts 02138

Received November 4, 1996<sup>⊗</sup>

**Abstract:** This work examines the influence of ions in solution on electroosmosis inside a fused silica capillary using capillary electrophoresis; it thereby examines “shielding” at charged interfaces. Theories are reviewed that model ionic solutions as continuous dielectrics: the nonlinear form of the Poisson–Boltzmann equation gives rise to the simplified, more commonly used Debye–Hückel (DH) equation. Capillary electrophoresis (CE) is used to measure the rate of electroosmotic flow as a function of the concentration of different monovalent and divalent cations in aqueous solution. These data are used to test three specific predictions of DH theory: this theory does not describe these data adequately. The central reason behind the inadequacy of DH theory here is its inability to account for details at the level of individual ions other than by mean-field electrostatics: that is, chemical characteristics of ions—for example, polarizability, hydrated size, energy of hydration, ability to coordinate other ions by chelation—are not accounted for. A model (the “dissociation model”) is described that treats the interactions between cations in solution and negatively charged groups on a surface in terms of discrete association equilibria with characteristic dissociation constants,  $K_d^{\text{eff}}$ . CE is then used as a tool to measure values of  $K_d^{\text{eff}}$  for different cations. These dissociation constants follow patterns that are consistent with ones that are familiar from studies in solution.

## Introduction

We have measured the shielding of siloxide ions ( $\text{SiO}^-$ ) at the surface of a fixed silica capillary as a function of the concentration and nature of ions in solution by measuring electroosmotic (EO) mobility,  $\mu^{\text{EO}}$ . We compare these experimental values of  $\mu^{\text{EO}}$  to those predicted using Debye–Hückel (DH) theory under conditions where DH theory is a valid approximation to the more complete Poisson–Boltzmann (PB) theory. We organize this paper conceptually into three parts. In the first part, we briefly review electroosmosis and examine the theory that leads to its description using both PB theory and DH theory. In the second part, we describe capillary electrophoresis as a convenient tool to examine three specific predictions of DH theory. We demonstrate that, in many cases, the experimental data are not described well by DH theory. We examine these three predictions over a range of concentrations that is consistent with the assumptions of DH theory, that is, concentrations at which the electrostatic potential at the charged surface of the capillary is less than  $\sim 25$  mV. In the third part, we introduce an empirical model for the electrostatic potential that incorporates ionic detail and describes the data well over the entire concentration range examined (0.005–500 mM). This second (dissociation) model treats the siloxide•cation interactions ( $\text{SiO}^- \text{M}^+$ ) as discrete, noncovalent association equilibria, with a characteristic dissociation constant,  $K_d^{\text{eff}}$  (much as for an acid–base dissociation). Many specific chemical properties of an ion may influence its interaction with another ion: the value of  $K_d^{\text{eff}}$  is a chemically convenient way of summarizing the collective influence of these interacting properties into a single number. The relative magnitudes of  $K_d^{\text{eff}}$  are consistent with chemical intuition.

## Theoretical Models for Electroosmosis

**Electroosmosis.** Electroosmosis is the motion of liquid driven by a combination of a *charge imbalance* at a solid–

liquid interface and an *electrical field* applied to that liquid (Figure 1). The liquid has finite viscosity and resists flow. The velocity of electroosmotic flow,  $\nu^{\text{EO}}$  ( $\text{m s}^{-1}$ ) results from a balance between electrical forces and viscous forces. Electroosmotic mobility,  $\mu^{\text{EO}}$  ( $\text{m}^2 \text{V}^{-1} \text{s}^{-1}$ ) is defined experimentally as the value of  $\nu^{\text{EO}}$  divided by the strength of the electrical field  $E$  ( $\text{V m}^{-1}$ ). This paper examines the influence of ions in solution on the value of  $\mu^{\text{EO}}$ . In this work, the solid is the interior, negatively charged surface of a hollow cylinder (capillary) composed of fused silica and the solution is aqueous and ionic. The charge imbalance at the surface of the capillary gives the solution a net charge, and the charged solution moves by electroosmosis in the uniform electrical field applied within the capillary.

We first describe in qualitative terms how we will examine the properties of the solution that affect  $\mu^{\text{EO}}$  (and  $\nu^{\text{EO}}$ ). In the section that follows this one, we will introduce some limited mathematical detail to make our qualitative arguments clear. As we will show later, changes in  $\mu^{\text{EO}}$  are directly proportional to changes in the “effective charge” at the surface of the capillary; because of charge neutrality, the effective charge at the surface is equal to the effective charge of the solution. This charged solution moves in bulk in a uniform electrical field. We examine the properties of the solution that influence this charge imbalance. Methods based on Poisson–Boltzmann (PB) theory do not directly or explicitly predict this charge imbalance.<sup>1</sup> Rather, PB theory is used to relate the *electrostatic potential* at the surface of the capillary ( $\Psi_0$ , volts) to the concentration of ions in solution ( $[\text{X}^\pm]$ , mol/L), the temperature ( $T$ , K), the dielectric constant ( $\epsilon$ , unitless), and the unshielded (naked) charge density ( $\sigma_0$ ,  $\text{C/m}^2$ ) at the surface.<sup>2–5</sup> This

(1) Healy, T. W.; White, L. R. *Adv. Colloid Interface Sci.* **1978**, *9*, 303–345.

(2) Smith, P. E.; Pettitt, B. M. *J. Phys. Chem.* **1994**, *98*, 9700–9711.

(3) Rashin, A. A.; Bukatim, M. A. *Biophys. J.* **1994**, *51*, 167–192.

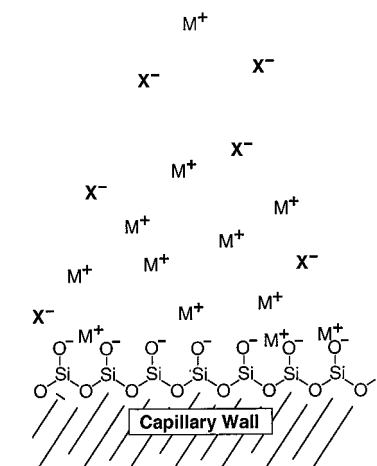
(4) Honig, B.; Sharp, K.; Yang, A. S. *J. Phys. Chem.* **1993**, *97*, 1101–1109.

(5) Rice, C. L.; Whitehead, R. *J. Phys. Chem.* **1965**, *69*, 4017–4024.

\* Author to whom correspondence should be addressed.

⊗ Abstract published in *Advance ACS Abstracts*, April 1, 1997.

## Distribution of Ions near a Charged Surface



## Debye-Hückel Model

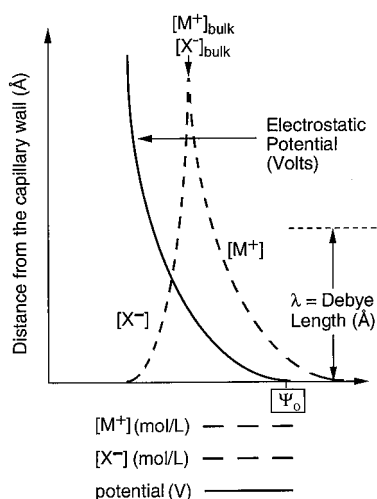


**Figure 1.** Schematic of the Debye–Hückel model for ionic solutions at charged interfaces. The Debye length,  $\lambda$ , is equal to  $\kappa^{-1}$ . The shapes of the curves are calculated. The potential at the wall is equal to  $\Psi_0$ .

potential and the viscosity of the solution are related to  $\mu^{\text{EO}}$  (through a combination of the Poisson–Boltzmann and Navier–Stokes equations).<sup>6,7</sup> The value of  $\sigma_0$  is the hypothetical charge that would exist at a given value of pH as the solution approaches that of water with no ions other than  $\text{H}^+$  and  $\text{OH}^-$ . This relationship between  $\Psi_0$ ,  $[\text{X}^\pm]_i$ , and  $\sigma_0$  requires two important assumptions: (i) electrostatic forces and thermal energy are the only important influences in the system and (ii) the molecular detail can be represented by a medium of continuous dielectric and continuous charge density.

**The Poisson–Boltzmann and Debye–Hückel Equations.** In this section, we examine in quantitative terms how  $\mu^{\text{EO}}$  is described theoretically by the PB and DH equations. The most successful model for describing the relationships among  $\Psi_0$ ,  $[\text{X}^\pm]_i$ , and  $\sigma_0$  is that of Poisson and Boltzmann; PB theory is expressed fundamentally as a second-order nonlinear differential equation (eq 1).<sup>2–5,8,9</sup> The charge on each ion is  $z_i e$ ,  $e$  is the charge on one proton (C),  $\epsilon$  is the dielectric constant (unitless),

(6) The value of  $\Psi_0$  is related conceptually, but not explicitly, to the magnitude of the charge imbalance; that is, the potential accounts (ostensibly) for so-called “shielding”.

(7) Fahien, R. W. *Fundamentals of Transport Phenomena*; McGraw-Hill: New York, 1983.

(8) Grahame, D. C. *Chem. Rev.* **1947**, *41*, 441–480.

(9) Parsons, R. In *Handbook of Electrochemical Constants*; Parsons, R., Ed.; Butterworths: London, 1954; Vol. 1, Chapter 3.

$$\epsilon\epsilon_0 \nabla^2 \psi_0 = -e \sum_i z_i [\text{X}^{\pm z_i}]_i \exp\left(\frac{-z_i e \psi_0}{kT}\right) \quad (1)$$

$$\frac{d^2 \psi}{dz^2} = \kappa^2 \psi \quad (2)$$

$$\psi_0 = \frac{\sigma_0}{\epsilon\epsilon_0 \kappa} \quad (3)$$

and  $\epsilon_0$  ( $\text{C}^2 \text{s}^2 \text{kg}^{-1} \text{m}^{-3}$ ) is the permittivity of free space. This equation can be solved for infinite, two-dimensional charged planes,<sup>10</sup> giving rise to the Gouy–Chapman–Stern–Grahame model, but cannot be solved analytically for the general case. In order to allow a general solution of eq 1, it is often linearized to eq 2 by series expansion of the exponential term, with truncation at the linear term. This approximation is valid as long as thermal energy is more important than electrostatic energy (i.e.,  $z\Psi e < kT \approx 0.6$  kcal/mol at room temperature, corresponding to  $\Psi < 25$  mV at room temperature for monocations).<sup>11</sup> The linearization increases in validity as the temperature increases. The solution of eq 2 gives the DH equation (eq 3), which relates the potential at the surface,  $\Psi_0$ , to  $\sigma_0$ ,  $\epsilon$ ,  $\epsilon_0$ , and the Debye parameter  $\kappa$  ( $\text{m}^{-1}$ ). The Debye parameter  $\kappa$  (eq 4) in turn relates the potential to the concentration of cations and anions in solution; the value of  $\kappa$  increases with increasing dielectric constant,  $\epsilon$ , concentration of cations  $[\text{M}^{n+}]$  (mol/L) of valency  $n$ , and concentration of anions  $[\text{X}^{m-}]$  (mol/L) of valency  $m$ , and decreases with increasing temperature  $T$  (K). Equation 4 also includes  $\epsilon_0$ ,  $k$  ( $\text{kg m}^2 \text{s}^{-2} \text{mol}^{-1} \text{K}^{-1}$ ),

$$\lambda = \frac{1}{\kappa} = \left[ \frac{\epsilon\epsilon_0 kT}{1000 N_A e^2 (n^2 [\text{M}^{n+}] + m^2 [\text{X}^{m-}])} \right]^{1/2} \quad (4)$$

the Boltzmann constant, and  $e$  (C), the elemental charge. The Debye length,  $\lambda$  (m) =  $1/\kappa$ , is loosely the distance away from a charged species at which electrostatic interactions with other charged species becomes negligible.

The value of  $\Psi_0$  is directly proportional to the electroosmotic mobility  $\mu^{\text{EO}}$  ( $\text{m}^2 \text{V}^{-1} \text{s}^{-1}$ ) with no assumption other than that the liquid obeys Stokes laws of viscous flow. The Navier–Stokes equation and the Poisson–Boltzmann equation combine to yield eq 5.<sup>5,7,12</sup>

$$\mu^{\text{EO}} = \frac{\epsilon\epsilon_0}{\eta} \psi_0 \quad (5)$$

Using the assumptions of DH theory, combination of eqs 3–5 yield an expression for  $\mu^{\text{EO}}$  (eq 6) that relates the value of  $\mu^{\text{EO}}$  theoretically to several variables: the value of  $\sigma_0$  ( $\text{C m}^{-2}$ ), the viscosity of the solution ( $\eta$ ,  $\text{kg m}^{-1} \text{s}^{-1}$ ), and the value of  $\kappa$  ( $\text{m}^{-1}$ ). The values of some of the parameters—especially that of  $\sigma_0$ —in eq 6 are unknown and are collapsed into a single system-dependent constant ( $C_{\text{DH}}$ ,  $\text{m s}^{-1} \text{mol}^{1/2} \text{L}^{-1/2}$ , eq 7).

$$\mu^{\text{EO}} = \frac{\epsilon\epsilon_0}{\eta} \psi_0 = \frac{\sigma_0}{\eta} \left[ \frac{\epsilon\epsilon_0 kT}{1000 N_A e^2 ([\text{M}^{n+}] n^2 + [\text{X}^{m-}] m^2)} \right]^{1/2} \quad (6)$$

(10) Equation 1 can be solved to yield  $\sigma_0 = (\epsilon\epsilon_0 kT / 2\pi e) \sin h(e\Psi_0/kT)$ .

(11) Grossman, P. D.; Colburn, J. C. *Capillary Electrophoresis: Theory and Practice*; Academic Press, Inc.: San Diego, 1992.

(12) Potocek, B.; Gas, B.; Kenndler, E.; Stedry, M. *J. Chromatogr.*, **A** **1995**, *709*, 51–62.

$$\mu^{\text{EO}} = \frac{\epsilon\epsilon_0}{\eta}\psi_0 = \frac{C_{\text{DH}}}{(n^2[M^{n+}] + \mu^2[X^{m-}])^{1/2}} \quad (7)$$

In this work, we examine the ability of DH theory (eq 7) to predict the *relative* experimental values of  $\mu^{\text{EO}}$ . In detail, we determined the value of  $C_{\text{DH}}$  by a fit to the observed data; that is, the values of  $C_{\text{DH}}$  were adjusted so that the values of  $\mu^{\text{EO}}$  predicted by eq 7 matched experimental values. This value of  $C_{\text{DH}}$  reflects the properties of the capillary and certain conditions (such as temperature) of the experiment that remain constant. We use this experimental value of  $C_{\text{DH}}$  to calculate value of  $\mu^{\text{EO}}$  for all ions at all concentrations. We later discuss the significant differences between observed and calculated values of  $\mu^{\text{EO}}$  for ions other than those used to set the value of  $C_{\text{DH}}$ .

#### Measurement of $\mu^{\text{EO}}$ Using Capillary Electrophoresis.

Capillary electrophoresis is a convenient experimental tool with which to examine electrostatic shielding and with which to test the theoretical models describing it. We measured the value of  $\mu^{\text{EO}}$  on a Beckman P/ACE System 5100 from the time of emergence of a neutral marker (*p*-methoxybenzyl alcohol, pMBA),  $t^{\text{neutral}}$  (s) according to eq 8. The lengths  $l_1$  (0.20 m) and  $l_2$  (0.27 m) are the distances along the unfused silica capillary (i.d. 50  $\mu\text{m}$ ) between the inlet and the detector, and the total length of the capillary, respectively, and  $V$  (V) is the applied voltage.<sup>13</sup>

$$\mu^{\text{EO}} = \frac{v^{\text{EO}}}{E} = \frac{l_1}{E t^{\text{neutral}}} = \frac{l_1 l_2}{V t^{\text{neutral}}} \quad (8)$$

#### Three Specific Predictions of DH Theory on Electroosmosis

Both PB and DH theories neglect molecular detail and assume that the solution can be treated as a continuous dielectric that interacts electrostatically with the charged surface. The DH equation (eq 5) makes three specific, testable predictions regarding the physical determinants of electroosmosis: (i) Cations of equal charge with a common anion will influence electroosmosis equally (for example, eq 7 predicts that equal concentrations of LiCl and CsCl will affect the value of  $\mu^{\text{EO}}$  equally). (ii) Cations of different charge with a common anion will influence electroosmosis differently (for example, eq 7 predicts that equal concentration of  $\text{MgCl}_2$  will decrease the value of  $\mu^{\text{EO}}$   $3^{1/2}$  to 1.7 times more than that of LiCl). (iii) Anions of different charge with a common cation will influence the electroosmosis differently (for example, eq 7 predicts that equal concentrations of  $\text{Li}_2\text{SO}_4$  will decrease the value of  $\mu^{\text{EO}}$   $3^{1/2}$  to 1.7 times more than LiCl); that is, DH theory predicts that changing the charge on the anion and on the cation affects electroosmosis in exactly the same way.

Figure 2 shows five sets of experimental data with five superimposed curves predicted from DH theory using eq 7. One theoretical curve was fit to the observed data for LiCl in order to estimate a value for the constant  $C_{\text{DH}}$ , taking into account the concentration of Tris cations ( $[\text{TrisH}^+] = 28 \mu\text{M}$ ) due to the Tris/Tris-HCl buffer.<sup>14,15</sup> We used the value of  $C_{\text{DH}}$  that best fit the data for LiCl in combination with eq 9 to calculate the relative positions of four more curves: the monocation  $\text{Cs}^+$  with  $\text{Cl}^-$ ; the divalent cation  $\text{Mg}^{2+}$  with  $\text{Cl}^-$ ; the divalent cation

(13) The conditions used during each CE experiment were as follows: voltage, 5000 V; current uncontrolled, but generally less than 10  $\mu\text{A}$ ; power (=current  $\times$  voltage) was less than 100 mW for all experiments; buffer, 50  $\mu\text{M}$  Tris/Tris-HCl (28  $\mu\text{M}$  Tris, 22  $\mu\text{M}$  Tris-HCl, pH = 9 at 25  $^\circ\text{C}$ ); detection, absorption at 214 nm; temperature  $25 \pm 0.2$   $^\circ\text{C}$ . We measured the time of emergence,  $t^{\text{neutral}}$  (s) for pMBA and calculated  $\mu^{\text{EO}}$  using eq 8.

(14) Tris is the trivial name for tris(hydroxymethyl)aminomethane and forms an effective buffer with its hydrochloride salt in the pH range 7–10.

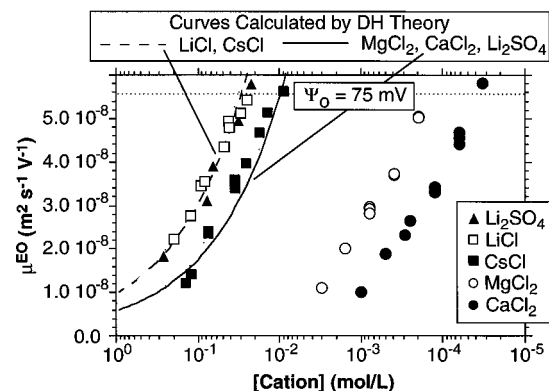


**Figure 2.** Predicted curves of Debye–Hückel theory relating  $\mu^{\text{EO}}$  to the concentration of different salts. We measured the value of  $\mu^{\text{EO}}$  using eq 8 as described in the text: 50  $\mu\text{M}$  Tris/Tris-HCl buffer, pH = 8.0,  $T = 25$   $^\circ\text{C}$ . The experimental data differ markedly from the five theoretical curves; the five curves appear as two due to superposition. Equation 5 is used to relate linearly the value of  $\mu^{\text{EO}}$  to that of  $\Psi_0$ . Although DH theory is explicitly valid for  $\Psi_0 < 25$  mV, the deviations appear to be pronounced only at  $\Psi_0 > 75$  mV.

$\text{Ca}^{2+}$  with  $\text{Cl}^-$ ; the divalent anion  $\text{SO}_4^{2-}$  with  $\text{Na}^+$ . Figure 2 shows that the five theoretical curves appear as two: the curves for the two monocations are coincident and the curves for the two divalent cations and the divalent anion are coincident. If we had used the data from a salt other than LiCl to set the value of  $C_{\text{DH}}$ , the relative positions of all five theoretical curves would be the same, but their absolute positions in the direction along the concentration axis would change.

DH theory inadequately describes the detailed influence of the ions we examined on the value of  $\mu^{\text{EO}}$  in our system (Figure 2). The primary reason that DH theory failed here is that it ignores all chemical detail of charged ions in solution interacting with an interface, thereby preventing a high density of charged  $\text{SiO}^-$  groups. We do not in this work suggest *which* chemical detail, but possible influences may include chelation, polarizability, specific dipole effects, specific induced dipole effects, extent of hydration, ionic size, etc. In principle, each of these types of non-electrostatic interactions could, in fact, be accounted for with perfect theoretical understanding of the different molecular properties: the expression for the energy corresponding to each type of interaction would be entered into the Boltzmann energy term in eq 1. As it is, only the electrostatic energy ( $z_i e \Psi_0$ ) appears as an energy term in the PB equation. In practice, the knowledge of a system is imperfect, and the energies of each of these terms (for example, polarizability and dipole terms) are very difficult to predict theoretically.

#### The Dissociation Model

A completely different approach would be to measure the charge imbalance at the surface *experimentally* and *directly* and not depend on the theoretical description that uses a potential. That is, we will assume that the “effective” charge at the surface,  $\sigma_{\text{eff}}$ , is precisely the charge imbalance that gives rise to electroosmosis. How does one measure “effective” surface charge experimentally and relate it to a parameter or parameters that can be considered intuitively on the basis of chemical experience? We propose that a model based on the discrete association and dissociation of metal–anion species at the

(15) As we discuss later in the text, some small concentration of buffer is needed in order to maintain a stable pH. All salts are very weak acids and bases, and the pH of water containing different salts is difficult to predict, unstable to small changes in temperature and atmospheric concentration of carbon dioxide.

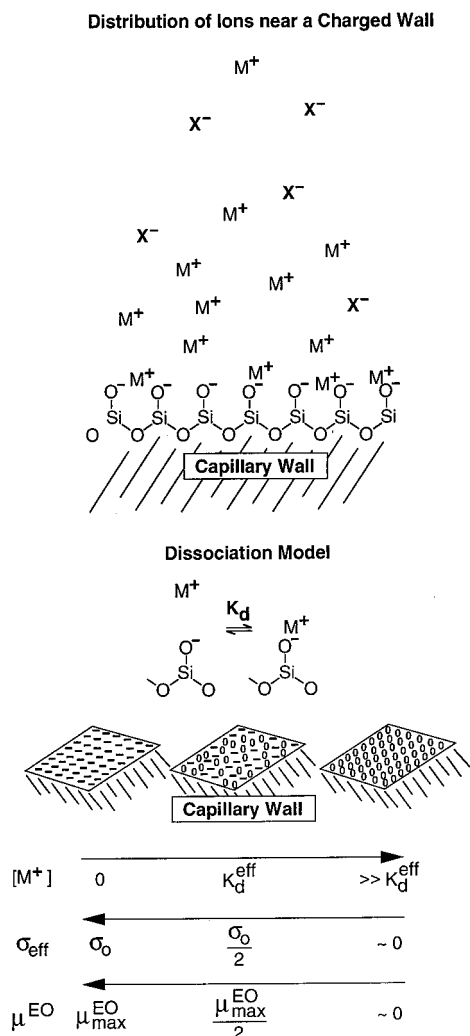
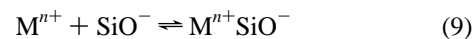


**Figure 3.** Schematic illustrations of some of the features of the dissociation model. The probable distribution of ions in solution are shown on the left; the essential feature of this system, the effective charge,  $\sigma_{\text{eff}}$ , changes as a function of the concentration of salt. The relation between  $[M^+]$  and  $\sigma_{\text{eff}}$  is given by  $K_d^{\text{eff}}$  (eqs 10–13). Changes in  $\sigma_{\text{eff}}$  are proportional to changes in  $\mu^{\text{EO}}$ .

solid–liquid interface can be used to achieve just this goal; such a model has been proposed earlier in crude form,<sup>1,16</sup> but has been largely ignored by both theoreticians and experimentalists. Stern has previously proposed that the first layer of ions at a charged surface—the so-called “Stern layer”—may behave differently than the second and higher layers due to chemical effects other than electrostatics, but proposed no method to examine these special features experimentally.<sup>1</sup>

**Qualitative Description of the Dissociation Model.** We first briefly describe the dissociation model using a minimum of equations, presenting the arguments and assumptions of the dissociation model in qualitative terms. In the section that follows this one, we introduce more quantitative definitions that we later use to interpret our experimental data.

We assume that there are two discrete states of the silanol groups on the surface of the capillary: an unassociated (free) state ( $\text{SiO}^-$ ) and associated (bound) state ( $\text{SiO}^-M^+$ ). The  $\text{SiO}^-$  contributes to the charge density on the surface, and the  $\text{SiO}^-M^+$  does not. The equilibrium is given by eq 9, and eq 10a defines the value of the effective dissociation constant,  $K_d^{\text{eff}}$  (Figure 3). We show later that one interpretation of  $K_d^{\text{eff}}$  is the



$$K_d^{\text{eff}} = \frac{[\text{SiO}^-][M^{n+}]}{[\text{SiO}^-M^{n+}]} \quad (10a)$$

$$\theta_{\text{SiO}^-} = \frac{[\text{SiO}^-]^\alpha}{[\text{SiO}^-M^{n+}]^\alpha + [\text{SiO}^-]^\alpha} \quad (10b)$$

concentration required to reduce electroosmotic flow by one-half (where the effective charge density on the surface,  $\sigma_{\text{eff}} = 1/2\sigma_0$ ).<sup>17</sup> The fraction of charged groups on the surface,  $\theta_{\text{SiO}^-}$  (unitless), may depend nonlinearly on the value of  $[\text{SiO}^-]$ : that is, the ions may bind cooperatively to the charged surface. Equation 10b defines a second empirical constant,  $\alpha$  (unitless), reflecting the cooperativity of association. If the value of  $\alpha < 1$ , then the association of cations with the charged surface occurs with negative cooperativity, and if the value of  $\alpha > 1$ , then this association occurs with positive cooperativity. We later describe  $\alpha$  and our definitions of cooperativity using more quantitative arguments.

In our model, the dependence of  $\mu^{\text{EO}}$  on the concentration of ions is not reflected in the value of  $\kappa$  but rather in the value of  $\sigma_{\text{eff}}$ ; the value of  $\sigma_{\text{eff}}$  varies as a result of coordination of cations in solution with siloxide ( $\text{SiO}^-$ ) groups on the wall of the capillary and neutralization of the fixed charge on the capillary. Increasing the concentration of a given cation increases the average number of bound siloxides, reduces the charge density on the wall, and consequently reduces the value of  $\mu^{\text{EO}}$ .

The  $K_d^{\text{eff}}$  represents an *average* value: the first cations to bind an initially highly negatively charged surface probably bind more tightly (with a lower, more favorable value of  $K_d$ ) than the last cations to bind an almost uncharged surface. Rigorously then, the interaction between the charged ions in solution and the charged groups on the surface should be considered using *two* empirical terms:  $K_d^{\text{eff}}$  value (the average value for all interactions at the surface) and  $\alpha$  (which we define quantitatively later in eqs 11–13). As we will show later, the experimental value of  $\alpha \approx 1/2$  for all salts that we examined in this work. This value is consistent with negative cooperativity and also consistent with the intuitive notion that the first cations to bind to the highly charged surface do so with higher affinity than the last cations. The cooperativity term is also, in principle, affected by chemical properties of the associating cations, such as its ability to bind to more than one  $\text{SiO}^-$  group simultaneously (chelation). At a given concentration of some ion, the values of  $K_d^{\text{eff}}$  and  $\alpha$  would be used to estimate directly the effective charge at the solid–liquid interface, and the resulting value of  $\mu^{\text{EO}}$ .

We are accustomed to modeling certain organic–inorganic interactions in terms of dissociation constants:  $\text{CH}_3\text{COO}^-$  and  $\text{H}^+$ ; calmodulin and  $\text{Ca}^{2+}$ , etc. We propose that the dissociation model reported here is equivalent conceptually to such dissociation constants; this model is related in some ways to theoretical models reported previously.<sup>1,18–20</sup> The values of  $K_d$  in our system differ in two ways from traditional “typical” dissociation constants. First, the values of  $K_d$  reported here are, in general, larger (that is, the binding is weaker;  $K_d > \text{mM}$ )

(17) Analogously, the effective dissociation constant of a polyacid is the concentration of  $\text{H}^+$  at which the polyacid is half-maximally charged ( $Z = 1/2Z_{\text{max}}$ ).

(18) Healy, T. W.; Yates, D. E.; White, L. R.; Chan, D. *J. Electroanal. Interfacial Electrochem.* **1977**, *80*, 57–65.

(19) Yates, D. E.; Levine, S.; Healy, T. W. *J. Chem. Soc., Faraday Trans. 1* **1974**, *70*, 1807–1815.

(20) Wiese, G. R.; James, R. O.; Yates, D. E.; Healy, T. W. *MTP Int. Rev. Sci.* **1965**, *6* (Electrochemistry).

(16) Huang, T. L.; Tsai, P. T.; Wu, C. T.; Lee, C. S. *Anal. Chem.* **1993**, *65*, 2887–2993.

than most values of  $K_d$  measured routinely by chemists and biochemists ( $K_d$  mM–pM). In principle, large values of  $K_d$  should not bother us. Second, the dissociation constants described here are *averages* of many dissociation constants. Acid–base titration of acidic or basic surfaces occur cooperatively and are nevertheless often described in terms of an average  $pK_a$ .<sup>21</sup> The dissociation model is exactly analogous to measuring characteristic values for the  $pK_a$  of particular groups either on charged solid–liquid interfaces<sup>22</sup> or within a polyacid (such as poly(acrylic acid)) in solution.

Chemists have sufficient experience that trends and magnitudes of these values of  $pK_a$  can be predicted *qualitatively* on the basis of the system and the conditions. For one example, the  $pK_a$  of trifluoroacetic acid ( $pK_a < 1$ ) is expected to be lower than that of acetic acid ( $pK_a \approx 4$ ). As a second example, we have shown previously that the average  $pK_a$  of a small dendrimeric molecule bearing nine carboxylates is greater ( $pK_a^{avg} \approx 6.5$ )<sup>23</sup> than that of acetic acid, as we would have predicted on the basis of chemical experience. We expect that this difference is due to electrostatic effects similar to those seen here: that is, we expect that the first dissociation of the nonacarboxylic acid (which removes a proton from a molecule bearing no charge) occurs more favorably than the ninth dissociation (which removes a proton from a molecule bearing eight negative charges). We show here with a limited data set that the dissociation constants of complexes between ions in solution and charged moieties on a surface follow trends that are consistent with chemical intuition, and trends and relative values of  $K_d^{eff}$  can be predicted without measurement.

**Quantitative Description of the Dissociation Model.** The value of  $\mu^{EO}$  is proportional to the charge imbalance (given by the effective charge density,  $\sigma_{eff}$ , C m<sup>-2</sup>) and inversely proportional to the viscosity of the solution ( $\eta$ , N m<sup>-2</sup> s<sup>-1</sup>) (eq 11). The proportionality constant is  $C_{diss}$  (m<sup>-1</sup> s<sup>-2</sup>). Both  $\mu^{EO}$

$$\mu^{EO} = \frac{C_{diss}}{\eta} \sigma_{eff} \quad (11)$$

$$\sigma_{eff} = \theta \sigma_o = \left( \frac{[SiO^-]^\alpha}{[SiO^-M^{n+}]^\alpha + [SiO^-]^\alpha} \right) \sigma_o \quad (12)$$

$$\mu_{[M^{n+}]}^{EO} = \frac{\frac{C_{diss}}{\eta} \sigma_o}{1 + \left( \frac{[M^{n+}]}{K_d^{eff}} \right)^\alpha} = \frac{\mu_{max}^{EO}}{1 + \left( \frac{[M^{n+}]}{K_d^{eff}} \right)^\alpha} \quad (13)$$

and  $\sigma_{eff}$  are dependent on the concentration of the cations in solution:  $\mu_{[M^{n+}]}^{EO}$  approaches its maximum value  $\mu_{max}^{EO}$  as  $\sigma_{eff}$  approaches its maximum value  $\sigma_o$  (Figure 3). The extent of ionization of the surface,  $\theta$  (unitless), relates  $\sigma_{eff}$  to  $\sigma_o$  (eq 12). The term  $\alpha$  accounts for any cooperativity (whether positive or negative) in the association of the cations in solution to the charged interface. We expect in general that most associations will be negatively cooperative ( $\alpha < 1$ ). Equation 13 follows from eqs 11–12 and expresses the relationship between the concentration of cation in solution and the effective dissociation constant.

(21) Kitagawa, S.; Tsuda, T. *J. Microcolumn Sep.* **1995**, *7*, 59–64.

(22) PB theory is often used to estimate the  $pK_a$  values of acidic and basic residues of a protein by means of modifying the  $pK_a$  of such a residue free in solution by a factor that depends on the magnitude and sign of the potential energy immediately around the residue on or in the protein.

(23) Mammen, M.; Gomez, F.; Whitesides, G. M. *Anal. Chem.* **1995**, *67*, 3526–3535.

**Experiments That Test the Dissociation Model.** To determine the value of  $K_d^{eff}$  for a particular ion experimentally (that is, to apply eq 13), we measure the electroosmotic mobility as a function of the concentration of that ion. The sequence of eqs 14a–c shows that  $K_d^{eff}$  is equal to the value of  $[M^{n+}]$  at which  $\mu^{EO}$  is reduced to half of its maximum value,  $1/2\mu_{max}^{EO}$  (Figure 3).

$$\mu_{[M^{n+}]}^{EO} = 1/2\mu_{max}^{EO} = \frac{\mu_{max}^{EO}}{1 + \left( \frac{[M^{n+}]_{1/2}}{K_d^{eff}} \right)^\alpha} \quad (14a)$$

$$\left( \frac{[M^{n+}]_{1/2}}{K_d^{eff}} \right)^\alpha = 1 \quad (14b)$$

$$K_d^{eff} = [M^{n+}]_{1/2} \quad (14c)$$

### Choosing a Range of Concentration of Salt to Examine.

Generally, it is not possible to perform the titration with salts over the maximum possible concentration range—that is, for value of  $[M^{n+}]$  ranging from 0 M to the solubility limit—for at least three major reasons: (i) A buffer is required to control the pH of the solution. We show later that this limitation places a *lower* bound on the value of  $[M^{n+}]$  that we can examine. (ii) The temperature of the solution within a capillary may increase due to Joule heating (defined as the heat produced as ions in a viscous solution move in an electrical field and dissipate energy). We show later that this limitation places an *upper* bound on the value of  $[M^{n+}]$  that we can examine. (iii) The viscosity of a the solution at a fixed temperature may increase as the concentrations of salt increases. We show later that this limitation also places a second *upper* bound on the value of  $[M^{n+}]$  that we can examine. In order to measure the influence of  $\sigma_{eff}$  on  $\mu^{EO}$  (that is, in order to use eq 10), we have to ensure that all other variables are constant during the measurement. The three most important variables that should remain constant over the entire concentration range of salt are pH, temperature, and viscosity. We discuss the influence of  $[M^{n+}]$  on the values of these three variables in the next three sections.

**(i) Limitation 1: Buffer.** This first limitation is only a limitation if the salt is itself nonbuffering. We first examine cases where the salt is buffering, for example, Tris base and its hydrochloride salt (Tris/Tris-HCl) and sodium phosphate salts. We measured the value of  $\mu^{EO}$  as a function of the concentration of both Tris/Tris-HCl and sodium phosphate at pH 8.0 (Figure 4). We were not able to examine concentrations below  $\sim 200$   $\mu$ M of phosphate due to an instability in the pH; we were able to explore concentrations as low as 6  $\mu$ M for Tris/Tris-HCl. Both sets of data were fit to eq 13, and the plateau corresponds to  $\mu^{EO} = \mu_{max}^{EO}$ , which is the maximum value in this capillary at zero concentration of all salts (distilled water at pH 8):  $\mu_{max}^{EO} = 1.13$  ( $10^{-7}$ ) m<sup>2</sup> V<sup>-1</sup> s<sup>-1</sup> for both buffers.

This first limitation was in general addressed by adding the smallest possible concentration of buffer that provided a stable pH over the entire concentration range of all salts examined. The Tris/Tris-HCl provides a stable pH at even 50  $\mu$ M (28  $\mu$ M TrisH<sup>+</sup>, 22  $\mu$ M Tris). At 8 mM, the TrisH<sup>+</sup> has shielded half of the charge on the wall of the capillary (Figure 4); at 28  $\mu$ M, this cation has shielded  $< 2\%$  of the charge. Even at this low concentration, the effect of *added* salts could not be analyzed at concentrations below which the portion of shielding due to buffer ions becomes significant. That is, we analyze the effect of added salts on electroosmotic flow only when  $K_d(M^{n+})/[M^{n+}] > K_d(\text{TrisH}^+)/[\text{TrisH}^+]$ . Later we show that a typical value of

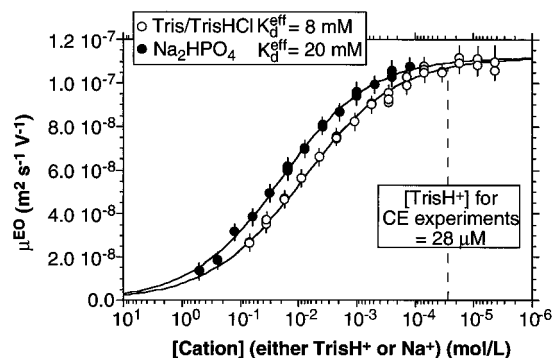


**Figure 4.** Electrophoretic mobility as a function of the concentration of the chloride salt of either  $\text{TrisH}^+$  or  $\text{Na}^+$ . The curves are fit to eq 13 to yield values of  $K_d^{\text{eff}}$  (see text for details). The two curves plateau at the same value of  $\mu^{\text{EO}} = 1.13 \times 10^{-7} \text{ m}^2 \text{ V}^{-1} \text{ s}^{-1}$ . The  $\text{pH} = 8.0 \pm 0.1$  at all concentrations of buffer; no salts other than buffer are present ( $T = 25^\circ\text{C}$ ). At  $[\text{Na}_2\text{PO}_4] < 200 \mu\text{M}$ ,  $\text{pH} < 7.8$ , and the data are therefore not shown.

$K_d$  for monocations is approximately 15 mM and that for divalent cations is approximately 0.05 mM; we therefore examined these two classes of salts at concentrations greater than 50 and 0.2  $\mu\text{M}$ , respectively.

**(ii) Limitation 2: Temperature.** We next examine the influence of  $[\text{M}^{n+}]$  on the temperature within the capillary during the experiment.<sup>24</sup> We wish to keep the temperature constant during the experiments for two reasons: values of  $K_d^{\text{eff}}$  may be dependent on the temperature and changes in temperature do affect the viscosity (independent of the effect of salts on the viscosity at a fixed temperature, which is a topic that we discuss in the next section). Heating of the solution within the capillary occurs due to the movement of ions through a viscous solution. The rate at which heat is generated is given by the power (voltage multiplied by current). At equilibrium the rate of heat generation is balanced by the rate of heat dissipation.

Our strategy for examining temperature changes inside the capillary is as follows: (i) We measure changes in conductivity of the solution as a function of temperature. (ii) We measure conductivity as a function of the power generated within the capillary. (iii) We combine the data from the first two measurements to infer an empirical relationship between changes in temperature and the amount of power generated.

**(a) Conductivity as a Function of Temperature.** The conductivity  $1/R$  ( $\Omega^{-1}$ ) is defined as the ratio of current  $I$  (A) to voltage  $V$  (V). The value of  $1/R$  for an ionic solution is dependent both on the ionic composition and the ionic strength of the solution and on the temperature. We first relate changes in  $1/R$  empirically to changes in temperature by holding ionic character (ionic strength and composition) constant. Here, we vary the temperature using a temperature bath and use the lowest possible voltage to measure conductivity (we assume that at this very low power output, Joule heating is negligible and show that this assumption is valid later). Figure 5a shows the results: we conclude that in our system, a change in temperature of 10  $^\circ\text{C}$  (from 25 to 35) causes a change in the conductivity of  $3 \times 10^{-10} \Omega^{-1}$ .

**(b) Conductivity as a Function of Power Generation.** We next examine the changes in  $1/R$  with increasing power output (that is, with increasing generation of heat); our ultimate goal is to relate temperature within the capillary to power output.

(24) The dielectric constant remains essentially constant for all solutions of NaCl at 25  $^\circ\text{C}$  in the concentration range of 1–200 mM and equals  $78.5 \pm 1$ . The value of the permittivity constant  $\epsilon_0 = 8.85 (10^{-12}) \text{ C}^2 \text{ N}^{-1} \text{ m}^{-2}$ . See: Tavares, M. F. M.; McGuffin, V. L. *Anal. Chem.* **1995**, *67*, 3687–3696.

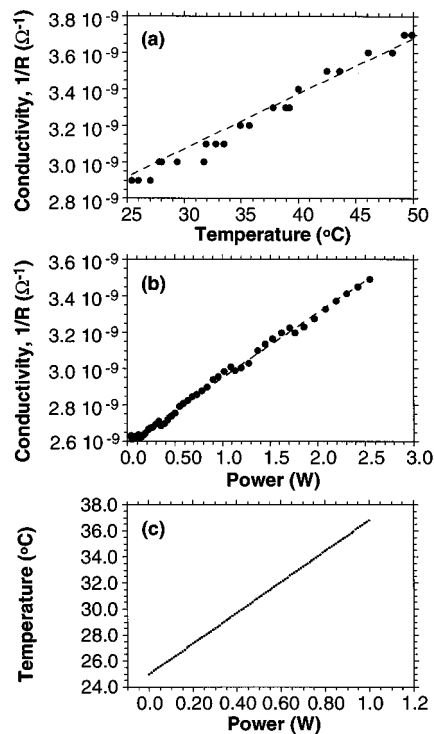


**Figure 5.** Conductivity as a function of power generation within a capillary or temperature: 50  $\mu\text{M}$  Tris buffer,  $\text{pH} = 8.0$ ,  $T = 25^\circ\text{C}$ . From the curves in a and b, we calculate the desired relation between power generation and temperature within the capillary (curve c). At power generations less than 100 mW, the change in temperature is  $< 1^\circ\text{C}$ . If no heat is generated within the capillary, the temperature inside of the capillary equals the temperature outside of the capillary,  $T = 25^\circ\text{C}$ .

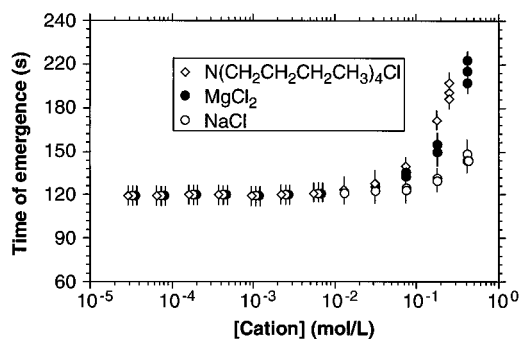
We examine the conductivity by varying the applied voltage and thereby varying the power,  $P$  ( $\text{W} = \text{J s}^{-1}$ ). Figure 5b shows that in our system, a watt causes a  $3 \times 10^{-10} \Omega^{-1}$  change in the value of  $1/R$ .

**(c) Temperature as a Function of Power Generation.** Combining the results shown in Figures 5a and 5b, we conclude that, for a 27 cm capillary used in conjunction with liquid cooling of the capillary, for every watt of power produced in the capillary, the temperature increases by  $\sim 10^\circ\text{C}$  (beginning at a 25  $^\circ\text{C}$  setpoint) (Figure 5c).

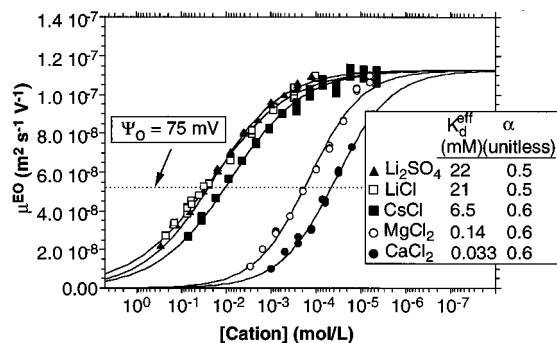
**(iii) Limitation 3: Changes in Viscosity.** Changes in viscosity can arise either due to changes in temperature (discussed in the previous section) or due to the presence of different concentrations of salts. It has been noted by others that the viscosity of a solution is largely independent of the concentration of simple salts.<sup>25</sup> Since we are examining salts that may not be “simple”, we investigate this possible influence next.

Figure 6 shows three examples that illustrate that the viscosity increases with increasing ionic strength. We have measured the changes in viscosity as a function of concentration of a range of different salts. The concentration at which viscosity begins to deviate from that of water by more than 5% places an upper limit on the concentration we can examine for that ion. This upper limit is reached at different concentrations depending on the nature of the salt. The following are three illustrative examples: viscosity increases by  $> 5\%$  at  $[\text{NaCl}] > 400 \text{ mM}$ ,  $[\text{MgCl}_2] > 100 \text{ mM}$ , and  $\text{Bu}_4\text{NCl} > 70 \text{ mM}$ .<sup>25</sup> Other consid-

(25) The kinematic viscosity has been previously recognized to remain constant over a wide range of salts at low to medium concentrations. For example,  $\eta = 0.8755 \pm 0.0017 \text{ cP}$  at 25  $^\circ\text{C}$  for aqueous solutions of NaCl in the concentration range of 1–100 mM. The value for  $\eta = 8.95(10^{-4}) \text{ kg m}^{-1} \text{ s}^{-1}$  for plain water at 25  $^\circ\text{C}$ .



**Figure 6.** Viscosity of aqueous solutions increases above that of pure water at high concentrations of salt. The time of emergence (s) of pMBA, where this time is linearly related to the viscosity of the solution, is measured as a function of the concentration of salt in solution using constant pressure (0.5 psi) pumping through a glass capillary (20 cm from inlet to detector, 27 cm total length, 50  $\mu\text{m}$  i.d.).



**Figure 7.** The dissociation model is used to fit the value of  $\mu^{\text{EO}}$  over a wide range of concentration of five different salts: 50  $\mu\text{M}$  Tris buffer, pH = 8.0,  $T = 25^\circ\text{C}$ . We calculated values of  $K_d^{\text{eff}}$  and  $\alpha$  based on best fits to eq 13.

**Table 1.** Effective Dissociation Constants and Cooperativity Terms for Various Cation-Siloxide Pairs<sup>a</sup>

| cation                  | anion              | $K_d^{\text{eff}}$ (mM) | $\alpha$ (unitless) |
|-------------------------|--------------------|-------------------------|---------------------|
| $\text{Li}^+$           | $\text{Cl}^-$      | $21 \pm 2$              | 0.5                 |
| $\text{Na}^+$           | $\text{Cl}^-$      | $19 \pm 2$              | 0.5                 |
| $\text{K}^+$            | $\text{Cl}^-$      | $8 \pm 1$               | 0.5                 |
| $\text{Et}_4\text{N}^+$ | $\text{Cl}^-$      | $9 \pm 1$               | 0.6                 |
| $\text{Bu}_4\text{N}^+$ | $\text{Cl}^-$      | $12 \pm 1$              | 0.6                 |
| $\text{Rb}^+$           | $\text{Cl}^-$      | $7 \pm 1$               | 0.6                 |
| $\text{Cs}^+$           | $\text{Cl}^-$      | $6.5 \pm 1$             | 0.6                 |
| $\text{Ca}^{2+}$        | $\text{Cl}^-$      | $0.033 \pm 0.004$       | 0.6                 |
| $\text{Mg}^{2+}$        | $\text{Cl}^-$      | $0.14 \pm 0.02$         | 0.6                 |
| $\text{Na}^+$           | $\text{Br}^-$      | $19 \pm 1$              | 0.5                 |
| $\text{Na}^+$           | $\text{I}^-$       | $20 \pm 1$              | 0.5                 |
| $\text{Li}^+$           | $\text{SO}_3^{2-}$ | $22 \pm 2$              | 0.5                 |
| $\text{Li}^+$           | styrene-sulfonate  | $21 \pm 2$              | 0.5                 |

<sup>a</sup> These values were obtained by fitting experimental data to eq 13.

erations, such as possible changes in temperature, which we discuss next, may further lower that upper limit.

In summary, to avoid changing any of the parameters in the experiment other than the effective charge at the wall, we examine concentrations of ions less than 200 mM at voltages less than or equal to 5 kV; at this concentration and this voltage, the power output (heat generation) is less than 200 mW, which we conclude (on the basis of the above discussion) results in a temperature change of less than  $2^\circ\text{C}$ .

We examine different salts over a wide range of concentrations, and use eq 13 to determine the values of  $K_d^{\text{eff}}$  (Figure 7). Table 1 gives some additional values of  $K_d^{\text{eff}}$  and  $\alpha$  for other salts. Dissociation constants of certain divalent metal-anion complexes have been measured previously (Table 2), and the

**Table 2.** Examples of Previously Measured Dissociation Constants<sup>a</sup>

| cation           | ligand | $K_d^{\text{eff}}$ (mM) |
|------------------|--------|-------------------------|
| $\text{Mg}^{2+}$ | ATP    | 0.091                   |
| $\text{Ca}^{2+}$ | ATP    | 0.17                    |
| $\text{Mn}^{2+}$ | ATP    | 0.018                   |
| $\text{Co}^{2+}$ | ATP    | 0.024                   |
| $\text{Mg}^{2+}$ | AMP    | 11                      |
| $\text{Ca}^{2+}$ | AMP    | 17                      |
| $\text{Mn}^{2+}$ | AMP    | 4.9                     |
| $\text{Co}^{2+}$ | AMP    | 2.6                     |
| $\text{Mg}^{2+}$ | Malate | 44                      |
| $\text{Ca}^{2+}$ | Malate | 16                      |
| $\text{Sr}^{2+}$ | Malate | 22                      |
| $\text{Zn}^{2+}$ | Malate | 2                       |

<sup>a</sup> Tabulated in *Biochemistry Handbook*. These values were measured at pH = 7 and in the presence (typically) of 100 mM NaCl. The charges on these ligands at pH = 7 are  $Z_{\text{ATP}} \approx -3.5$ ,  $Z_{\text{AMP}} \approx -1.5$ , and  $Z_{\text{Malate}} \approx -2$ .

values and trends of  $K_d$  in these systems is consistent with the values measured here.

## Discussion

Dissociation models have been applied to the reinterpretation of certain colligative properties.<sup>26</sup> The model suggesting that the first layer of ions may be different from subsequent layers of ions is also old: first introduced by Stern,<sup>21</sup> first examined by Healy,<sup>1</sup> and used by Huang<sup>16</sup> and others.<sup>21,27</sup> These studies introduced the idea that the Stern layer can behave differently from the subsequent layers, but have not developed these ideas into testable form. These studies did not, for instance, offer measurements of dissociation constants or a means of doing so. The two major goals of this work were to provide a theoretical basis for the dissociation model and to describe capillary electrophoresis as a convenient tool to estimate the dissociation constants between different metal ions and charged groups on surfaces.

The experimental data based on measurements of EO flow fit the prediction of a dissociation model better than DH theory in three regards. First, the dependence of  $\mu^{\text{EO}}$  on the concentration of cations is predicted accurately over a greater range of concentrations of ions by the dissociation model than by DH theory. Second, the observed dependence of  $\mu^{\text{EO}}$  on the nature of the cation is accounted for in the dissociation model by an effective dissociation constant ( $K_d^{\text{eff}}$ ) for cation-siloxide complexes at the wall; DH theory predicts no specific dependence on the ions. Third, a large dependence of  $\mu^{\text{EO}}$  on the charge of the soluble anions ( $X^{n-}$ ) is not observed, as would be predicted by DH theory; the dissociation model predicts only a small influence.<sup>28,29</sup> The underlying reasons that these observations are not predictable using DH theory are that it considers the solution as a continuous dielectric and ignores all contributions to interactions other than electrostatics.

We feel the application of a dissociation model to electrostatic shielding has been largely ignored in the literature for two main reasons. First, the continuum theory is (in certain manifestations) easy to use and has successfully rationalized many of the trends central to the field of electrostatics. This theory has the attractive feature that it does not require experimental data.

(26) Heyrovska, H. *A Reappraisal of Arrhenius' Theory of Partial Dissociation of Electrolytes*; Heyrovska, H., Ed.; American Chemical Society: Washington, DC, 1989; Vol. 390, Chapter 6.

(27) Salomon, K.; Burgi, D. S.; Helmer, J. C. *J. Chromatogr.* **1991**, 559, 69–80.

(28) Atamna, I. Z.; Metral, C. J.; Muschik, G. M.; Issaq, H. J. *J. Liq. Chromatogr.* **1990**, 16.

(29) Green, J. S.; Jorgenson, J. W. *J. Chromatogr.* **1989**, 478, 63–69.

Second, there remains no easy, systematic way (until capillary electrophoresis) to measure some of the *molecular* influences of electrostatic shielding. The dissociation model has the disadvantage that it requires measurement; the PB and DH approaches are completely theoretical. The dissociation model has a number of advantages including the ability to detect detailed chemical effects: chelation, interactions involving polarization and other close range electrostatic effects, effects due to the extent of hydration and ionic size, and effects due to the entropy of the processes involved. Qualitative patterns emerge in this limited set of data, and these dissociation constants that are consistent with chemical intuition. For example, the values of  $K_d^{\text{eff}}$  decrease in the order  $\text{Li}^+ > \text{Na}^+ > \text{K}^+ > \text{Rb}^+ > \text{Cs}^+$  (and also  $\text{Mg}^{2+} > \text{Ca}^{2+}$ ), which is consistent with both the trend in polarizability and hydrated (but not ionic) radius. That is, as these cation become smaller and more polarizable, they tend to bind more tightly to the charged groups on the glass surface. Also, the values of  $K_d^{\text{eff}}$  decrease in the order  $\text{Me}_4\text{N}^+ > \text{Et}_4\text{N}^+ > \text{Bu}_4\text{N}^+$ , which is consistent with the trend in ionic (and hydrated) radius. We do not, in this work, examine in detail the reasons *why* the dissociation constants are different for different cations of the same charge or *why* the difference between a typical divalent cation and a typical monocation is much greater than predicted by DH theory. That is, we do not attempt to rationalize the details of the chemical influences on electrophoretic mobility but rather show that there *are* chemical influences. Qualitative trends in these influences (given quantitatively by the dissociation constants) are qualitatively predictable without measurement, much like the  $\text{p}K_a$  values of many acids and bases.

Interesting effects of the influence of radially applied electrical fields on the rate of electroosmotic flow have been described

previously (that is, electroosmosis can be slowed and even reversed by placing the silica capillary inside electrically conductive sleeves that are then charged).<sup>30,31</sup> Although we do not examine such external influences directly in this work, our model accommodates these effects by adding a constant to eq 13.

Capillary electrophoresis may be useful for the study of specific ionic influences of effective charge in biological systems. For example, the effective charge on the surface of a platelet may not depend simply on the ionic strength but on the detailed arrangement of acid groups on the surface of the platelet (for example,  $\gamma$ -carboxylated glutamic acid groups) and on the presence and concentration of specific ions such as  $\text{Ca}^{2+}$  and  $\text{Mg}^{2+}$ . Biological interactions may be examined in which electrostatic interactions may contribute to the total energy of interaction between a ligand and a receptor: the extent to which electrostatics plays a role in these systems may not, once again, depend *simply* on the ionic strength of the medium but also on the specific ions present. Capillary electrophoresis may be a useful tool with which to examine association of ions common to biological systems (i.e.,  $\text{Na}^+$ ,  $\text{K}^+$ ,  $\text{Cl}^-$ ,  $\text{Ca}^{2+}$ ,  $\text{Mg}^{2+}$ , and phosphate) with a range of charged surfaces and charged molecules such as DNA and proteins.

**Acknowledgment.** This work was supported by the NIH, Grant GM 51559. E.E.S. and M.M. thank Eli Lilly for predoctoral fellowships.

JA9638115

(30) Lee, C. S.; McManigill, D.; Wu, C.-T.; Patel, B. *Anal. Chem.* **1991**, *63*, 1519.

(31) Hayes, M. D.; Kheterpal, I.; Esing, A. G. *Anal. Chem.* **1993**, *65*, 2407.